AD-A174 647 CARBON FIBER MICROELECTRODES AS SUBSTRATES FOR MERCURY FILMS(U) STATE UNIV OF NEW YORK AT BUFFALO DEPT OF CHEMISTRY 25 SEP 86 TR-13 N00014-84-K-0052 1/1

UNCLASSIFIED F/G 9/1 NL

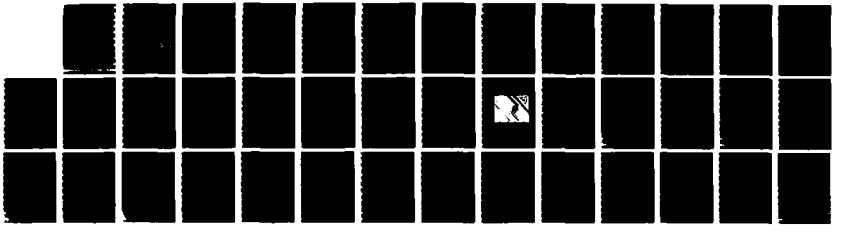

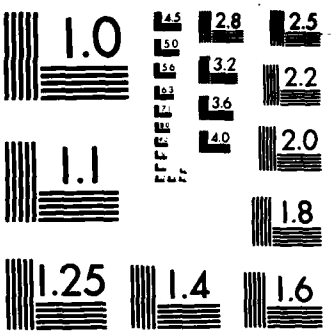

MICROCOPY RESOLUTION TEST CHART
NATIONAL BUREAU OF STANDARDS-1963-A

SECURITY CLASSIFICATION OF THIS PAGE (When Data Entered)

REPORT DOCUMENTATION PAGE		READ INSTRUCTIONS BEFORE COMPLETING FORM
1. REPORT NUMBER: Technical Report No. 13	2. GOVT ACCESSION NO.	3. RECIPIENT'S CATALOG NUMBER
4. TITLE (and Subtitle): Carbon Fiber Microelectrodes as Substrates for Mercury Films		5. TYPE OF REPORT & PERIOD COVERED: (12)
		6. PERFORMING ORG. REPORT NUMBER
7. AUTHOR(s): J. Golas and Janet Osteryoung		8. CONTRACT OR GRANT NUMBER(s): N00014-84-K-0052
9. PERFORMING ORGANIZATION NAME AND ADDRESS: Department of Chemistry, State University of New York at Buffalo, Buffalo, New York 14214		10. PROGRAM ELEMENT, PROJECT, TASK AREA & WORK UNIT NUMBERS: NR 051-855
11. CONTROLLING OFFICE NAME AND ADDRESS: Office of Naval Research, Chemistry Program, Arlington, Virginia 22217		12. REPORT DATE: September 25, 1986 13. NUMBER OF PAGES: 39
14. MONITORING AGENCY NAME & ADDRESS (if different from Controlling Office)		15. SECURITY CLASS. (of this report): Unclassified 15a. DECLASSIFICATION/DOWNGRADING SCHEDULE

16. DISTRIBUTION STATEMENT (of this Report)

Approved for Public Release: Distribution Unlimited.

17. DISTRIBUTION STATEMENT (of the abstract entered in Block 20, if different from Report)

18. SUPPLEMENTARY NOTES

Accepted for publication in Analytica Chimica Acta.

19. KEY WORDS (Continue on reverse side if necessary and identify by block number)

carbon fibers, mercury films, anodic stripping voltammetry, microelectrodes

20. ABSTRACT (Continue on reverse side if necessary and identify by block number)

Conditions for mercury deposition at cylindrical carbon fiber microelectrodes were examined and presented together with a new construction of electrode body and the manner in which the fiber is held. Data obtained in KSCN and acetate buffer solutions suggest that in order to obtain linear dependence of square wave stripping peak vs. mercury concentration the amount of the deposit should not exceed few monolayers. This could be caused by surface inhomogeneity as confirmed by electron microscopy and by the limited amount of mercury that can be (Continued)

DD FORM 1 JAN 73 1473 EDITION OF 1 NOV 65 IS OBSOLETE

SECURITY CLASSIFICATION OF THIS PAGE (When Data Entered)

quantitatively deposited at the surface. Several remarks on lead deposition "in situ" are also given.

OFFICE OF NAVAL RESEARCH

Contract N00014-84-K-0052

Task No. NR 051-855

TECHNICAL REPORT NO. 13

Carbon Fiber Microelectrodes as Substrates for Mercury Films

by

Janusz Golas and Janet Osteryoung

Published in

Analytica Chimica Acta

State University of New York at Buffalo
Department of Chemistry
Buffalo, New York 14214

September 25, 1986

Carbon Fiber Microelectrodes as Substrates for Mercury Films

J. Golas[a] and Janet Osteryoung*

Department of Chemistry

SUNY at Buffalo

Buffalo, NY 14214

[a]Permanent Address: Academy of Mining and Metallurgy, Institute of Material Science, 30-059 Kraków, Poland

A-1

Summary

Conditions for mercury deposition at cylindrical carbon fiber microelectrodes were examined and presented together with a new construction of electrode body and the manner in which the fiber is held. Data obtained in KSCN and acetate buffer solutions suggest that in order to obtain linear dependence of square wave stripping peak vs. mercury concentration the amount of the deposit should not exceed few monolayers. This could be caused by surface inhomogeneity as confirmed by electron microscopy and by the limited amount of mercury that can be quantitatively deposited at the surface. Several remarks on lead deposition "in situ" are also given.

Introduction

Several papers have been published recently on different types of carbon fiber microelectrodes [1-4]. Edmonds has reviewed this and related work in the context of the properties of the carbon fibers [5]. This material seems to indicate that carbon fibers can be used either directly as carbon electrodes or as a base material for mercury film electrodes. Although the results obtained with carbon fibers are still sometimes difficult to compare with each other, probably due to variability of the starting material and different pretreatment procedures, the increasing volume of experimental data followed by some theoretical considerations [6,7] is bringing carbon fibers closer to the point of general practical application. Three types of carbon fiber electrodes have been used: 1) the exposed single fiber with cylindrical geometry; 2) single fibers or arrays of fibers embedded in an insulator and having disk geometry; and 3) brushes, or arrays of exposed fibers. The first two seem to offer the best possibilities as voltammetric electrodes. Behavior of these electrodes depends on dimensions and shape and also on the properties of the material. Diffusion and convection are difficult to control or reproduce with the brush configuration [2].

Procedures for fabricating carbon fiber microelectrodes are improving [1,8,9], which should encourage and simplify further investigations. We present below an improvement over our previous procedure for making exposed carbon fiber microelectrodes [9]. The main aim of this paper is to indicate limitations of exposed carbon fibers for mercury deposition and for *in situ* deposition of lead. Relations between the properties of the apparent film of lead amalgam and the resulting cyclic voltammograms of lead are also presented.

Although relatively long (ca. 8-10 mm) cylindrical carbon fiber electrodes, which are the subject of this paper, at first sight may seem to be less practical, because fragile, than corresponding disk electrodes, they in fact have several advantages. They are much less sensitive to imperfect seal between electrode and insulator than are disk electrodes, because the integrated current density in the vicinity of the seal is a minute fraction of the total. Non-planar diffusion at an exposed fiber depends on the radius of the fiber rather than its length, so electrode area and properties of cylindrical diffusion can be controlled independently, again in contrast to the disk. In particular, the length of the fiber can be adjusted to give the desired total current for a given type of experiment. Finally, the exposed fiber electrodes make it possible to investigate the properties of the surface of the cylinder as an electrode, which might be different from those of the crossection.

Experimental Section

Instrumentation and Reagents

An IBM electrolytic cell was used along with a three electrode system in which carbon fiber, platinum and saturated calomel electrodes were used as working, counter and reference electrodes, respectively. Two voltammetric techniques were used: square wave voltammetry (SWV) and staircase voltammetry (SCV). All voltammetric measurements were performed with a computer-controlled potentiostat based on a Digital Equipment Corp. PDP-8/e minicomputer [10]. Some additional coulometric measurements were carried out using an EG&G PARC Model 173 Potentiostat and with Model 179 Digital Coulometer.

Reagents were of analytical grade and distilled water passed through a Millipore "Milli Q" purification system was used for preparation of the solutions. The following solutions were used as supporting electrolytes: 0.1 M KSCN (pH = 2.5; acidified with HNO_3), acetate buffer (1.25 M KOAc, 1.7 M HOAc, pH = 4.6), 0.1 M KNO_3. The proper amounts of 0.05 M $Hg(NO_3)_2$ and 0.01 M $Pb(NO_3)_2$ were added to a chosen supporting electrolyte using Eppendorf pipets.

Solutions were purged with argon for about 7 min before each experiment; after purging the argon flow was directed over the solution . All experiments were run in quiet solutions without stirring. According to our previous experience stirring during deposition causes the fiber to move which worsens reproducibility of stripping analysis.

Electrodes - Construction and Preliminary Tests

The working electrodes were made from 8 μm-diameter carbon fibers (AESAR, Johnson Matthey Inc.). The procedure for making the electrode is based on an idea which involves sealing the fiber into a matrix of tygon and

heat-shrinkable tubing [7]. Gentle heating of the tip of the electrode with a soldering iron melts the inner tygon tube and shrinks the outer tube about the fiber and molten tygon. The main change from the procedure of Ref [7] is the Teflon body and glass support, as shown in Fig. 1. This body enables very quick replacement of the fiber in the case of damage and improves protection against breaking by providing the additional support which holds the tip of the fiber.

It should be noted that fibers even from the same manufacturer differ according to the smoothness of the surface. There are also different shapes of cross sections (e.g. AESAR fibers are circular whereas Celion GY-70 is bilobal). An electron-micrograph of AESAR carbon fibers is presented in Fig. 2. The surface is randomly covered with small dimples which did not disappear after pretreatment. The standard pretreatment procedure included cleaning in a solution of Alconox detergent in an ultrasonic bath, rinsing with water, cleaning again in HNO_3:H_2O (1:4) solution in the ultrasonic bath, rinsing with water, and finally drying. The last step was a moderate electrooxidation at +0.3 V for 1 min.

In principle, after cleaning one could select the proper part of the best-looking fiber by microscopic examination, but this procedure would be too time-consuming to yield practical electrodes. Furthermore, there is considerable uncertainty regarding what properties might be desirable to optimize performance in voltammetric experiments. A series of experiments were carried out on different fibers to examine the quantitative variability from fiber to fiber. Four carbon fibers were used for deposition of mercury and the resulting square wave anodic stripping voltammograms were compared for four deposition times (10, 20, 40, 100s), two deposition potentials (-0.6, -1.0 V) and several concentrations of

Hg(II) in the range 1-80 μM in 0.1 M KSCN. Although the results for each particular fiber are reproducible for deposition for a given time and concentration of Hg(II) (usually three repeated scans gave identical curves) different results were obtained for different fibers. For illustration representative data are presented in Table I. These electrochemical results suggest that the heterogeneous appearance of the surfaces shown in Fig. 2 in fact reveal differences in surface properties which affect electrochemical behavior.

Based on this preliminary series of experiments we chose one of those electrodes for further investigations. This was the carbon fiber microelectrode of length 9.06 mm (by microscopic measurement) and area of 0.228 mm^2. This electrode was then successfully used for several months without any damage. All of the following data were obtained using this one electrode.

Results and Discussion

Mercury has been deposited on carbon fiber surfaces but it has not been established how much mercury can be deposited quantitatively. Following previous results [9] we investigated more carefully the conditions for mercury deposition in three different electrolytes: potassium thiocyanate, acetate buffer and potassium nitrate. The results in the first two supporting electrolytes are discussed together because they are qualitatively the same, whereas the nature of the mercury deposition in KNO_3 is a bit more complex. A series of depositions were run at E_d = +1.0 V for t_d = 10, 20, 40 or 100s in the range of Hg(II) concentration from 1-80 μM. The observed dependence of anodic stripping peak current density on mercury concentration in 0.1 M KSCN and in acetate buffer is shown in Figs. 3 and 4, respectively.

At sufficiently low concentration of Hg(II) or short deposition time, stripping peak current depends linearly on concentration of Hg(II), but at higher concentrations or longer times the dependence is less strong. This is more obvious for 0.1 M KSCN solution, where in general we obtained approximately three times larger stripping peaks than for acetate buffer under the same conditions. As a result in 0.1 KSCN the curves of Figure 3B become non-linear at values of concentration smaller than those of Figure 4B.

In order to estimate the amount of deposited mercury at which this effect starts, we measured charge consumed during each deposition. There is not a sharp boundary between the linear and non-linear ranges. We defined the boundary region as that in the range of conditions between 40 μM Hg(II) with 10s deposition and 20 μM Hg(II) with 100s deposition. The mean values for five replicate measurements were the following: $Q = 4.37$ μC ($S_x = 0.34$ μC) for [Hg(II)] = 20 μM; $Q = 0.99$ μC ($S_x = 0.02$ μC) for [Hg(II)] = 40 μM. It is well-known that deposits of mercury on carbon substrates are not coherent films but rather exist as collections of puddles or droplets [9]. We have observed such deposits on carbon fiber electrodes. However, bearing this in mind, it is useful to calculate the effective film thicknesses corresponding to these values of charge. Using $\ell = 9.06$ mm and $r = 4$ μm, the critical range of thickness of the deposit corresponding to these values of charge is 3-14 Å. Using a value of 1.44 Å as the atomic radius of Hg, these numbers suggest that the stripping peak current depends linearly on coverage only up to a few monolayers.

At higher coverages reproducibility of the anodic stripping peak worsens, the peak becomes wider and more flat, and even the peak area (which should be proportional to total charge) does not depend linearily on

deposition time. The latter point is shown in Fig. 5. Examples were taken of two different concentrations of Hg(II) and two different deposition times. As is seen in Fig. 5, for values of $i_p w_{1/2}/A$ (peak current density times width at half height) in the range 5-10 $\mu A \cdot V/mm^2$ the dependence on deposition time decreases. This range of values again corresponds to an average thickness of several angstroms, agreeing with the results of Figs. 3 and 4. The same trends characterized by the same critical numbers occured in acetate buffer. Therefore this effect is due to the surface of the carbon fiber itself, and is not due only to the special characteristics of thiocyanate ion.

Similar experiments were performed in 0.1 M KNO_3. Some typical anodic stripping voltammograms are shown in Fig 6. Peak current is linear with concentration of Hg(II) up to concentrations for which the second peak appears. But the currents are 10-20 times smaller than those obtained in thiocyanate or acetate solution. The results are qualitatively the same with added nitric acid (pH≥2.5). Clearly the deposition of mercury is hindered and the stripping process is complicated in this medium. The equilibrium constant for the reaction of Hg^{2+} with Hg to form Hg_2^{2+} is 88 [14]. Equilibrium for this reaction is established rapidly, so in the vicinity of the electrode when Hg is present the major form in solution should be Hg_2^{2+}. The anions SCN^-, CH_3COO^-, NO_3^- all form insoluble salts of the composition Hg_2X_2. In the case of SCN^-, the Hg(II) oxidation state is stabilized by formation of $Hg(SCN)_4^{2-}$. The equilibrium constant for the reaction $Hg_2(SCN)_2(s) + 2SCN^- = Hg(SCN)_4^{2-} + Hg$ is 1 L/mol [14], and therefore in 0.1 M KSCN one would expect no precipitation of $Hg_2(SCN)_2(s)$ in the presence of Hg for concentrations of Hg(II) less than 0.01 M. For acetate, again HgX_4^{2-} is the predominant form, and the equilibrium constant

for the disproportionation reaction is sufficiently large that no precipitate should form [14-16]. Nitrate is quite different. The solubility product of $Hg_2(NO_3)_2 \cdot 2H_2O(s)$ estimated from the enthalpy values of Ref [14] is given by log K = -57 $(mol/L)^3$. (It is "well-known", however that $Hg_2(NO_3)_2$ is quite soluble in slightly acid aqueous solution). Stabilization of Hg(II) by complex formation is negligible [17]. Therefore the undesirable behavior of mercury deposits in nitrate media appears due to the presence of Hg(I) and may reflect local precipitation of a form of $Hg_2(NO_3)_2$ in the vicinity of the electrode.

Anodic stripping of codeposited lead. The following series of experiments was carried out to test the range of conditions suitable for in situ codeposition of lead. The solution was 0.1 M KSCN (pH = 2.5) with [Hg(II)] = 40 μM. Deposition was carried out without stirring for 60s at -0.6V. The nominal thickness of the mercury deposit under these conditions is 18 Å. After deposition anodic square wave voltammograms were obtained with E_{SW} = 25 mV, ΔE_s = 6 mV, and f = 100 Hz. The electrode was conditioned before each deposition for 1 min at +0.3 V. The procedure was repeated for varied concentrations of lead. Anodic stripping peak current increases linearly with concentration of lead up to 4 μM. This is shown in Fig. 7. However, at [Pb(II)] = 1 μM, the anodic stripping peak for Hg is diminished and shifted to more negative potential, and this effect is systematically more pronounced, the higher the concentration of Pb(II). An example is shown in Fig. 8. The solubility of Pb in Hg is 0.013 mol Pb/mol Hg. The molar ratio of Pb to Hg in the amalgam under the conditions of this experiment, assuming deposition is diffusion-controlled, is just the concentration ratio, [Pb(II)]/[Hg(II)]. In the present case [Hg(II)] = 40 μM, so saturation should occur for [Pb(II)] $\geq$ 0.5 μM. We observe the first

diminution in the Hg-stripping peak at [Pb(II)] ≈ 1 μM. It is well-established that saturation must be avoided to obtain acceptable results for anodic stripping voltammetry [11-13]. In the present case the calibration curve remains linear up to a concentration of ca 8x the saturation value. For concentrations of Pb(II) greater than about 8 μM (~15x the saturation value) we obtained broader anodic stripping peaks between -0.4 and -0.5 V and no peak for stripping of Hg. This effect has been reported previously for Cd [9].

Finally we would like to present few observations on the practical use of mercury coated carbon fiber microelectrodes. Fig. 9 presents two cyclic staircase voltammograms, both obtained in thiocyanate solution with Hg(II) concentration 40 μM and Pb(II) concentration 1.2 mM. Curve 1 (Fig 9) was obtained on a clean fiber, whereas curve 2 was obtained using a mercury-coated fiber (deposit thickness of ~95Å).

The voltammogram is improved dramatically in the presence of the mercury deposit. We have not found reports on experiments with similar conditions. Presently the theoretical basis for treating this problem, which involves aspects of cylindrical diffusion, nucleation and growth, and thin films, does not exist. However the practical implications for developing analytical methods suggest that this phenomenon should be examined in much greater detail.

Conclusions

Although an exposed carbon fiber by itself is not convenient to operate with, the proposed construction of electrode body and the manner in which the fiber is held seems to ensure easy replacement of the fiber and makes the electrode relatively durable. Electron microscopic pictures of carbon fibers show a significant discrimination of the surface which could cause the differences in results while using different fibers. The applied pretreatment procedure did not affect significantly the surface properties.

According to our results, mercury can be deposited on carbon fibers, but stripping peak height depends linearly on mercury concentration only when the amount of deposit is less than a few monolayers. There are also some limitations for lead deposition "in situ". The best results are obtained for approximately 20Å-thickness of the Hg deposit. The anodic stripping peak height increases linearly with lead concentration in the solution until the extent of supersaturation for the lead-mercury amalgam exceeds about seven times the value of saturation. The results obtained by using cyclic staircase voltammetry for lead on mercury-coated carbon fibers indicate that their quality is very sensitive to thickness of the mercury deposit. The best-shaped curves were obtained for deposits in the nominal thickness range of 50÷150Å.

This result depends on the properties of the material, its dimensions, and possibly the vertical position of the electrode.

References

1. M. R. Cushman, B. G. Bennett and C. W. Anderson, Anal. Chim. Acta 130 (1981) 323.

2. G. Schultze and W. Frenzel, Anal. Chim. Acta 159 (1984) 95.

3. M. A. Dayton, J. C. Brown, K. J. Stutts and R. M. Wightman, Anal. Chem. 52 (1980) 946.

4. V. J. Jennings and J. E. Morgan, Analyst. 110 (1985) 121.

5. T. E. Edmonds, Anal. Chim. Acta, 175 (1985) 1-22.

6. K. Aoki, K. Honda, K. Tokuda and H. Matsuda J. Electroanal. Chem. 182 (1985) 267.

7. K. Aoki, K. Honda, V. Tokuda and H. Matsuda J. Electroanal. Chem. 186 (1985) 79.

8. J. L. Ponchon, R. Cespuglio, F. Gonon, M. Jouvet and J. F. Pujol, Anal. Chem., 51 (1979) 1483.

9. J. Golas and J. Osteryoung, in press.

10. T. R. Brumleve, J. J. O'Dea, R. A. Osteryoung and J. Osteryoung, Anal. Chem. 53 (1981) 702-706.

11. M. T. Kozlovskii, A. J. Zebreva and V. P. Gladyshev, Amalgamy i ikh Primienene, Alma-Ata, 1971.

12. Z. Stojek, B. Stepnik, Z. Kublik, J. Electroanal. Chem. 74 (1976) 277.

13. T. R. Copeland and R. K. Skogerboe, Anal. Chem., 46 (1974) 1257A.

14. "Standard Potentials in Aqueous Solution, A. J. Bard, R. Parsons, and J. Jordon, Eds.; International Union of Pure and Applied Chemistry, 1985. Marcel Dekker, New York.

15. "Stability Constants of Metal-ion Complexes: Part B. Organic Ligands. IUPAC Chemical Data Series-No. 22. D. D. Perrin, Ed. Pergamon, Oxford, 1979.

16. "Atlas of Metal-Ligand Equilibria in Aqueous Solution," J. Kragsten, Ellis Horwood, Chicester, 1978.

17. "Critical Stability Constants Vol. 4: Inorganic Complexes," R. M. Smith and A. E. Martell, Plenum, New York, 1976.

Table I

Peak current density for square wave anodic stripping voltammograms[a]

	i_p/A, $\mu A/mm^2$			
A, mm^2	0.265	0.279	0.164	0.228[b]
E_d, V				
-0.6	33.32	21.33	46.16	44.96
-1.0	132.23	75.98	153.35	116.01

[a]Solution: 80 μM Hg(II) in 0.1 M KSCN; deposition time: 40 s; square wave parameters: ΔE_s = 4 mV, E_{sw} = 25 mV, f = 100 Hz. The four different electrodes are identified by their areas.

[b]This electrode taken for further investigations.

Figure Captions

Fig. 1. Schematic drawing of the cylindrical carbon fiber microelectrode.

Fig. 2. Electron-microscopic picture of a bunch of the AESAR carbon fibers.

Fig. 3. A. Anodic stripping square wave voltammograms of mecury in 0.1 M KSCN, pH = 2.5. Square wave parameters: E_{sw} = 24 mV, ΔE_s = 4 mV, f = 100 Hz. E_d = -1.0 V, t_d = 40 sec. [Hg(II)]: 1) 8, 2) 20, 3) 40, 4) 80 μM.

B. Dependence of anodic stripping square wave peak current density on Hg(II) concentration for varied deposition time. t_d(s) = (o) 10, (▲) 20, (△) 40, (●) 100. Other conditions those of Figure 3A.

Fig. 4. A. Anodic stripping square wave voltammograms of mercury in 1.25/1.7 M acetate buffer pH = 4.6. [Hg(II)]: 1) 20, 2) 40, 3) 80 μM. Other conditions as in Figure 3A.

B. Dependence of anodic stripping square wave peak current density on mercury concentration for varied deposition time: (○) 10, (▲) 20, (△) 40, (●) 100 s.

Fig. 5. Anodic stripping square wave voltammetry of mercury in 0.1 M KSCN. The dependence of peak area on deposition time. [Hg(II)] = 20 μM, E_d = -0.6 V (▲) or -1.0 V (△); [Hg(II)] = 80 μm, E_d = -0.6 V (○) or -1.0 V (●). Peak area approximated as height times width at half height, $w_{1/2}$.

Fig. 6. Anodic stripping square wave voltammograms of mercury in 0.1 M KNO_3 [Hg(II)] (μM): 1) 8, 2) 20, 3) 40 (Fig. 6A) and 160 (Fig 6B). Other conditions as Fig. 3A.

Fig. 7. Anodic stripping square wave voltammetry of lead codeposited with mercury. Dependence of peak height on concentration of lead. (E_d = -0.6V; t_d = 60 s; SWV: E_{sw} = 24 mV, ΔE_s = 4 mV, f = 100 Hz; 0.1 M KSCN, pH = 2.5. [Hg(II)] = 40 μM. Straight line fitted to linear portion; correlation coefficient = 0.9992.

Fig. 8. Anodic stripping square wave voltammograms of mercury (curve 1) and mercury/lead amalgam (2). [Pb(II)] = 2.5 μM. Other conditions as Fig. 7.

Fig. 9. Cyclic staircase voltammograms (sweep rate 0.8 V/sec) Solution: 0.1 M KSCN, pH = 2.5, [Hg(II)] = 0.04 mM, [Pb(II)] = 1.2 mM. Curve 1 without previous mercury deposition. Curve 2 mercury deposited at -0.3V. Apparent thickness of the deposit ≈ 95 Å.

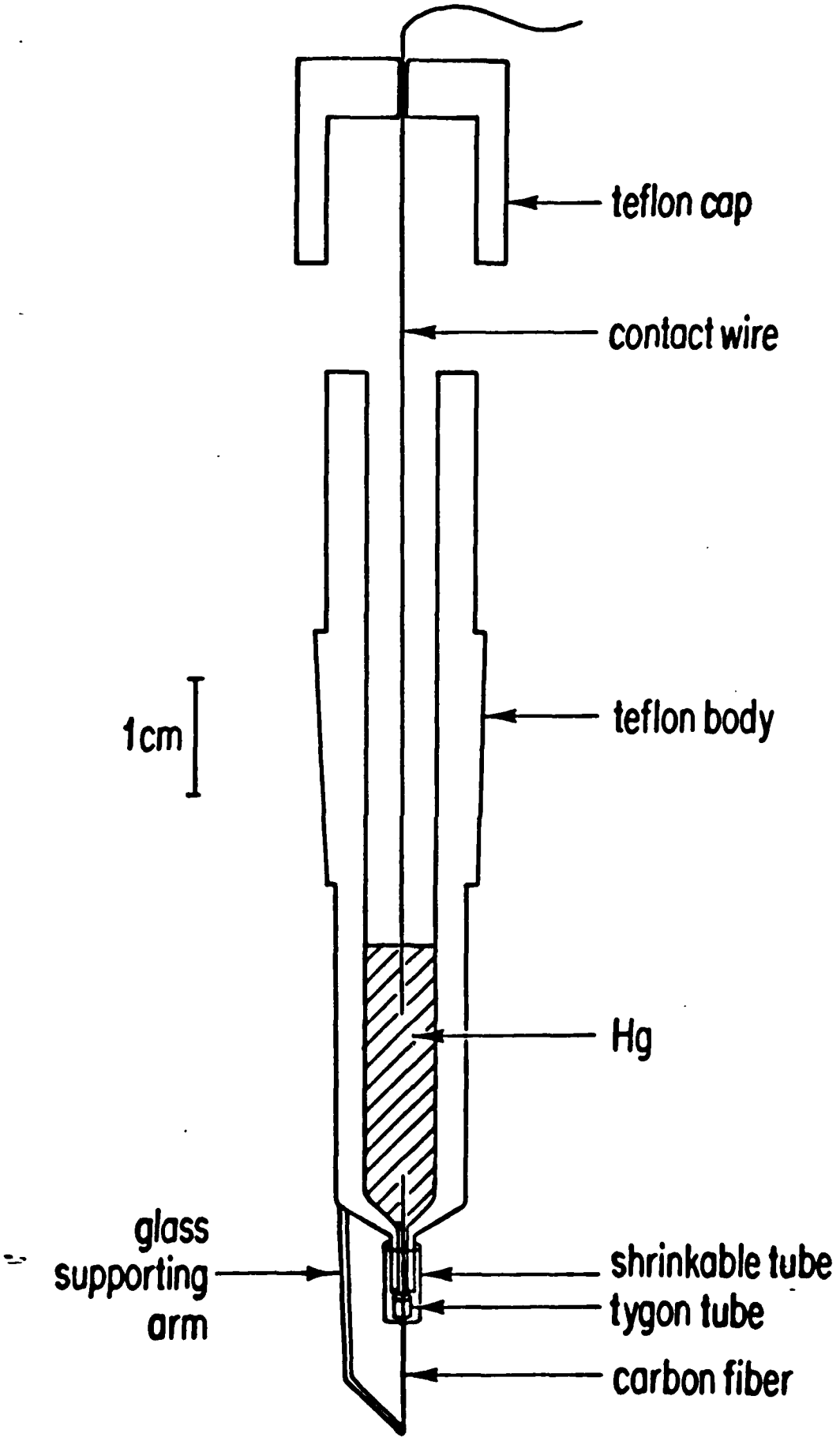
teflon cap
contact wire
1cm
teflon body
Hg
glass
supporting
arm
shrinkable tube
tygon tube
carbon fiber

FIGURE 1

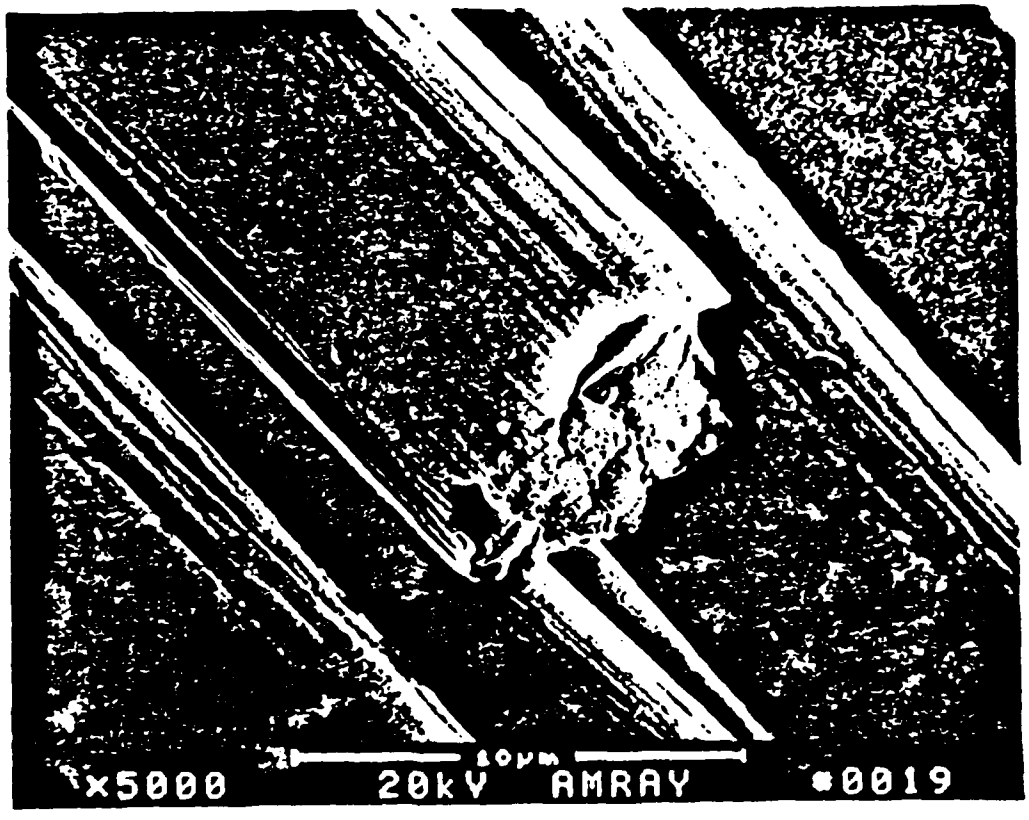

FIGURE 2

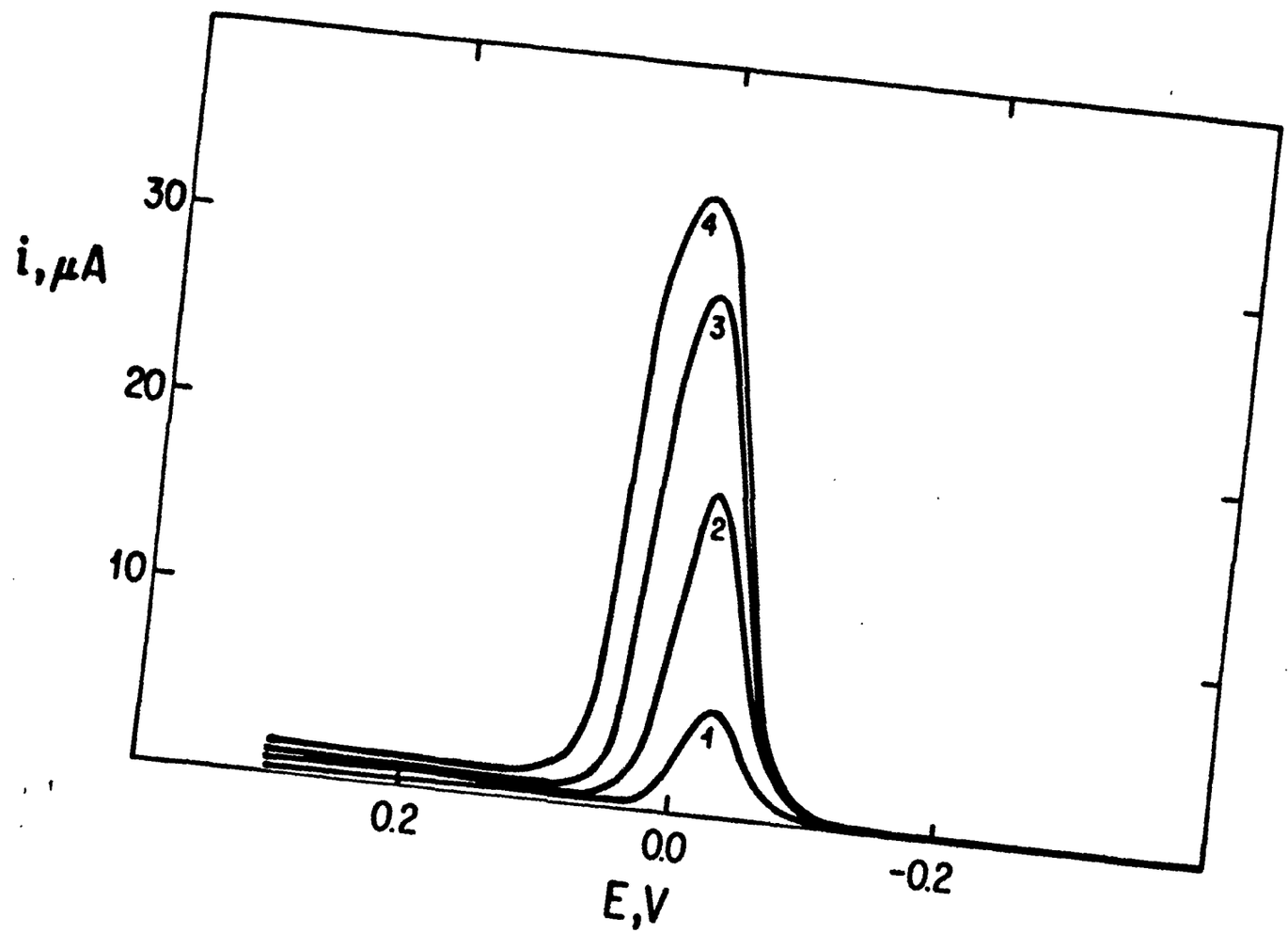

FIGURE 3A

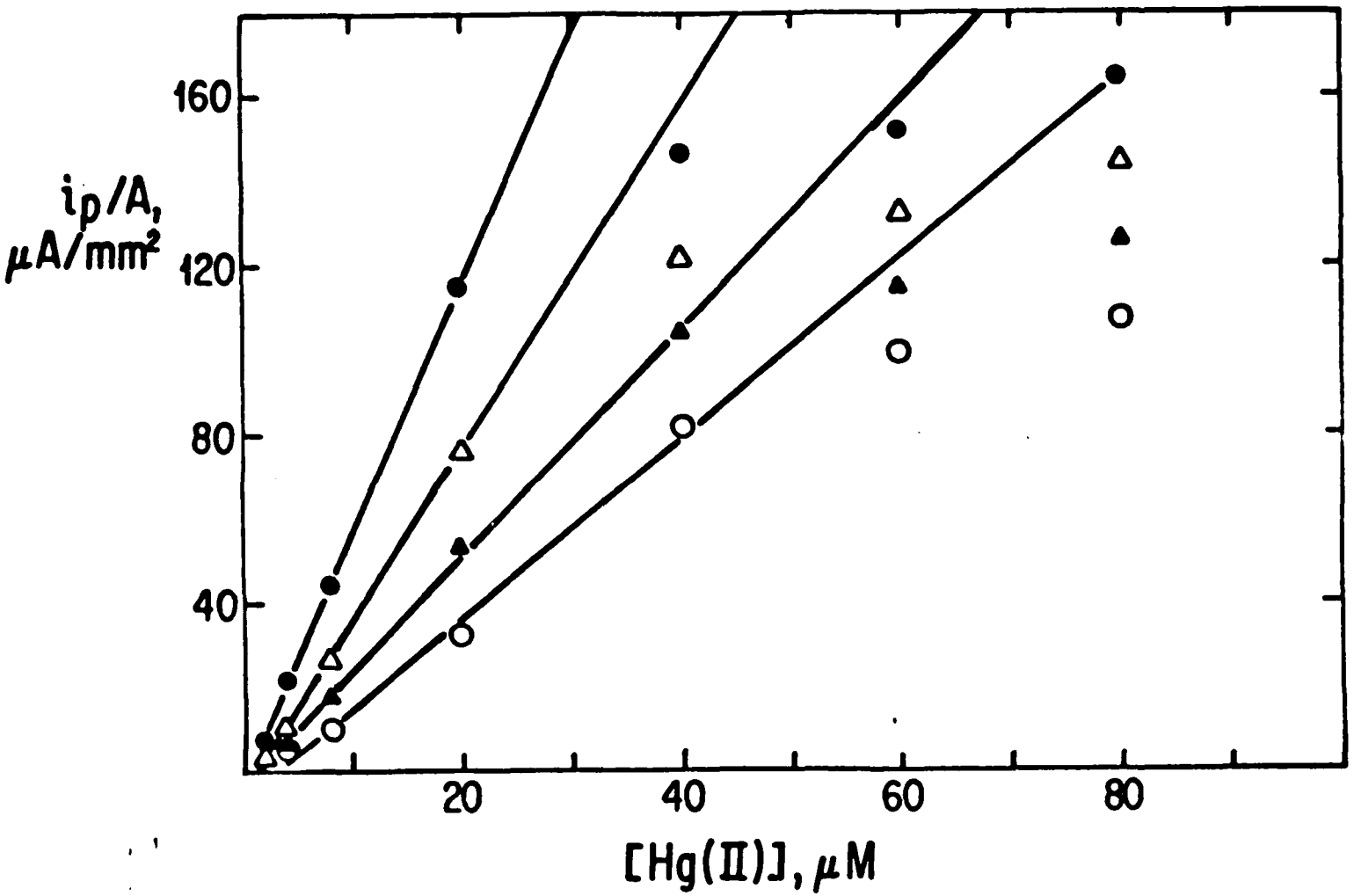

FIGURE 3B

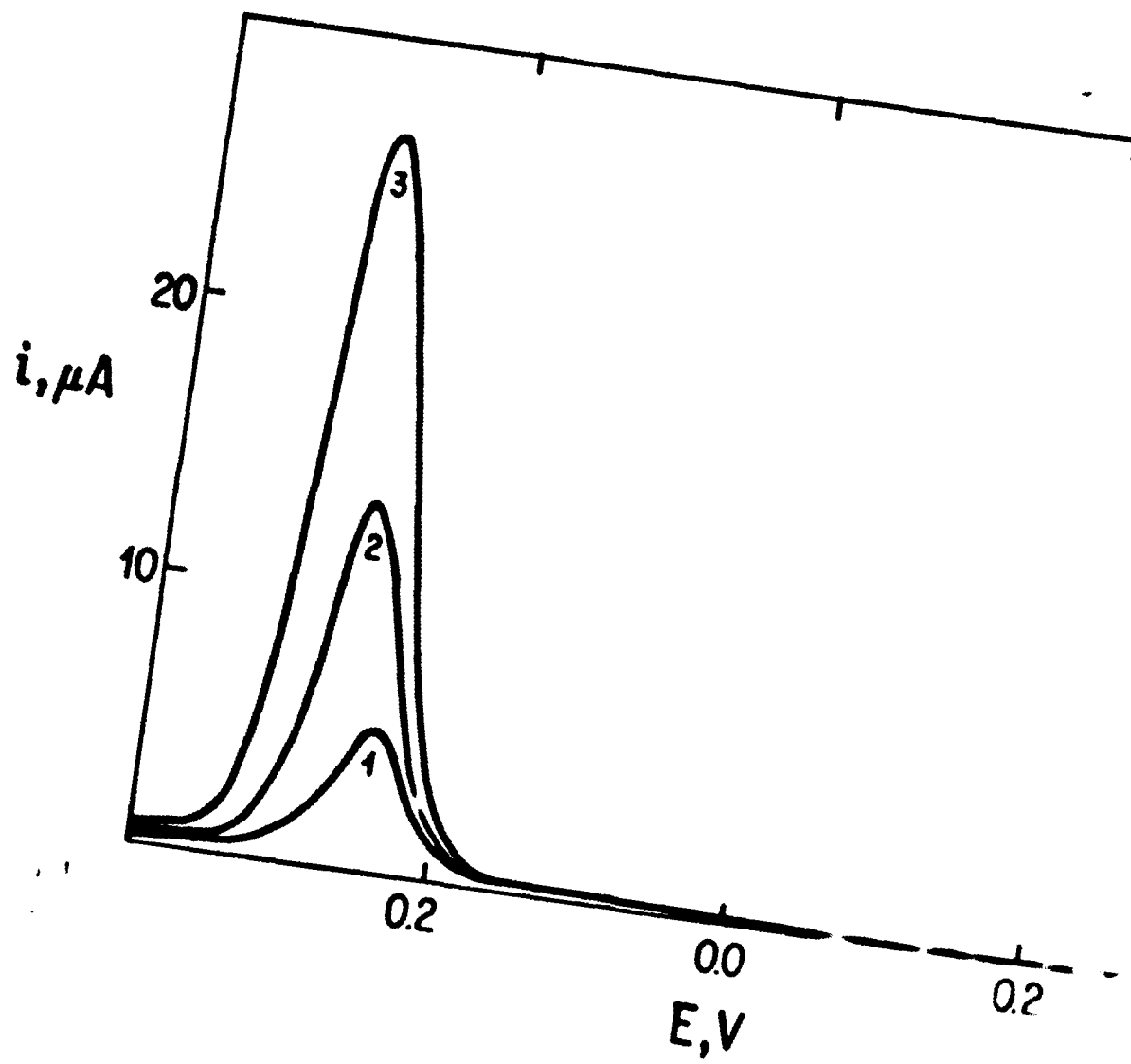

FIGURE 4A

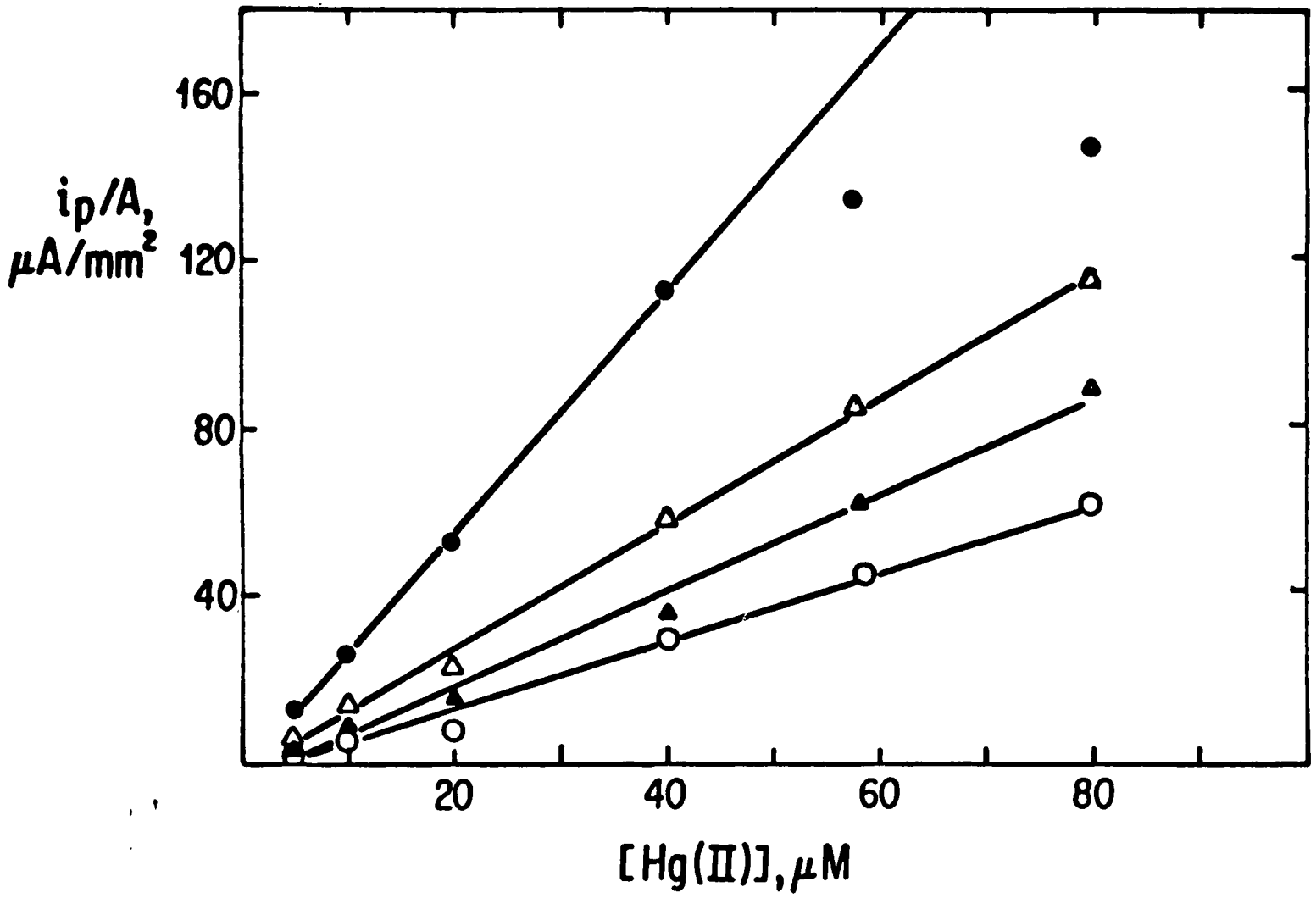

FIGURE 4B

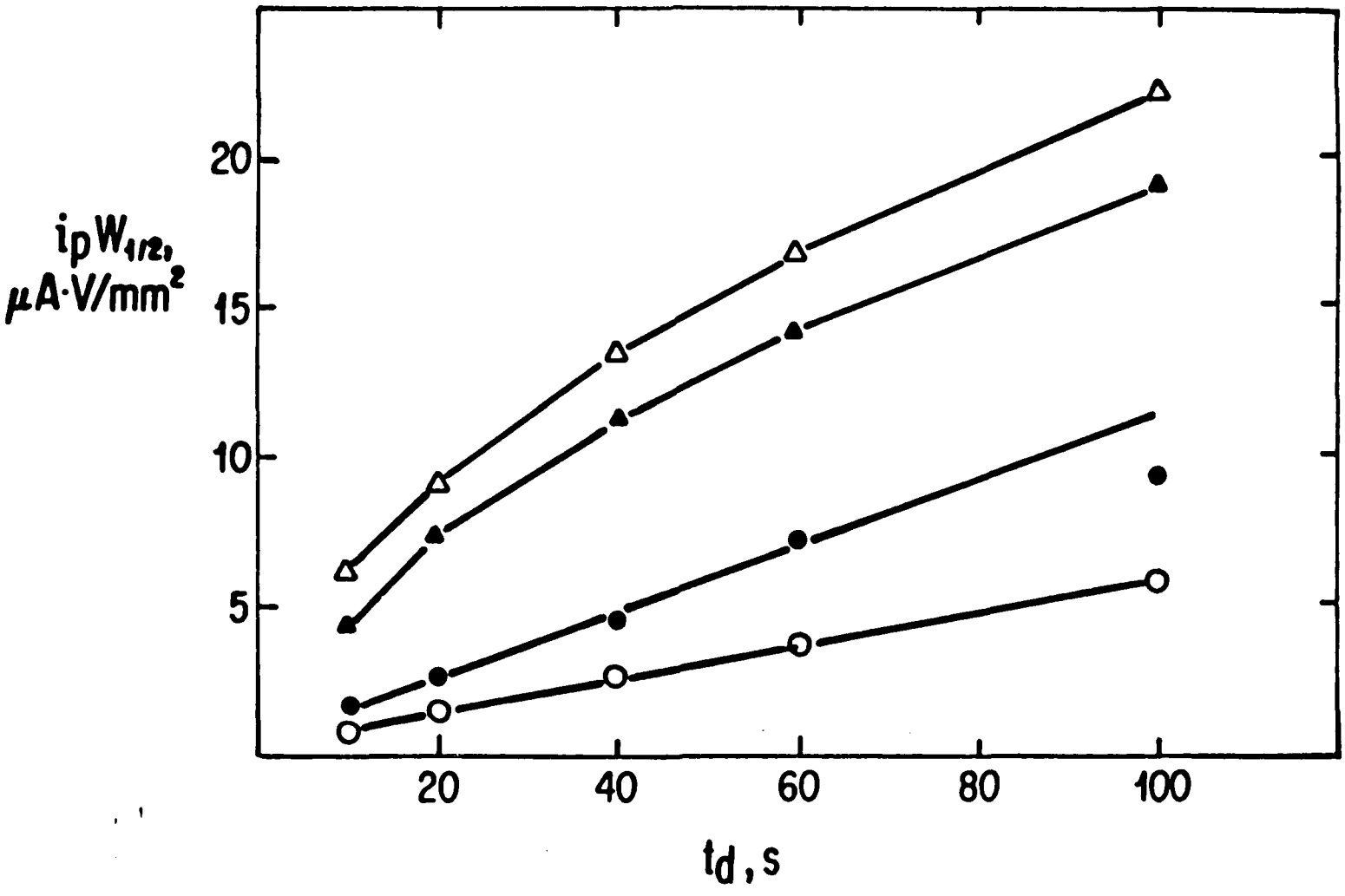

FIGURE 5

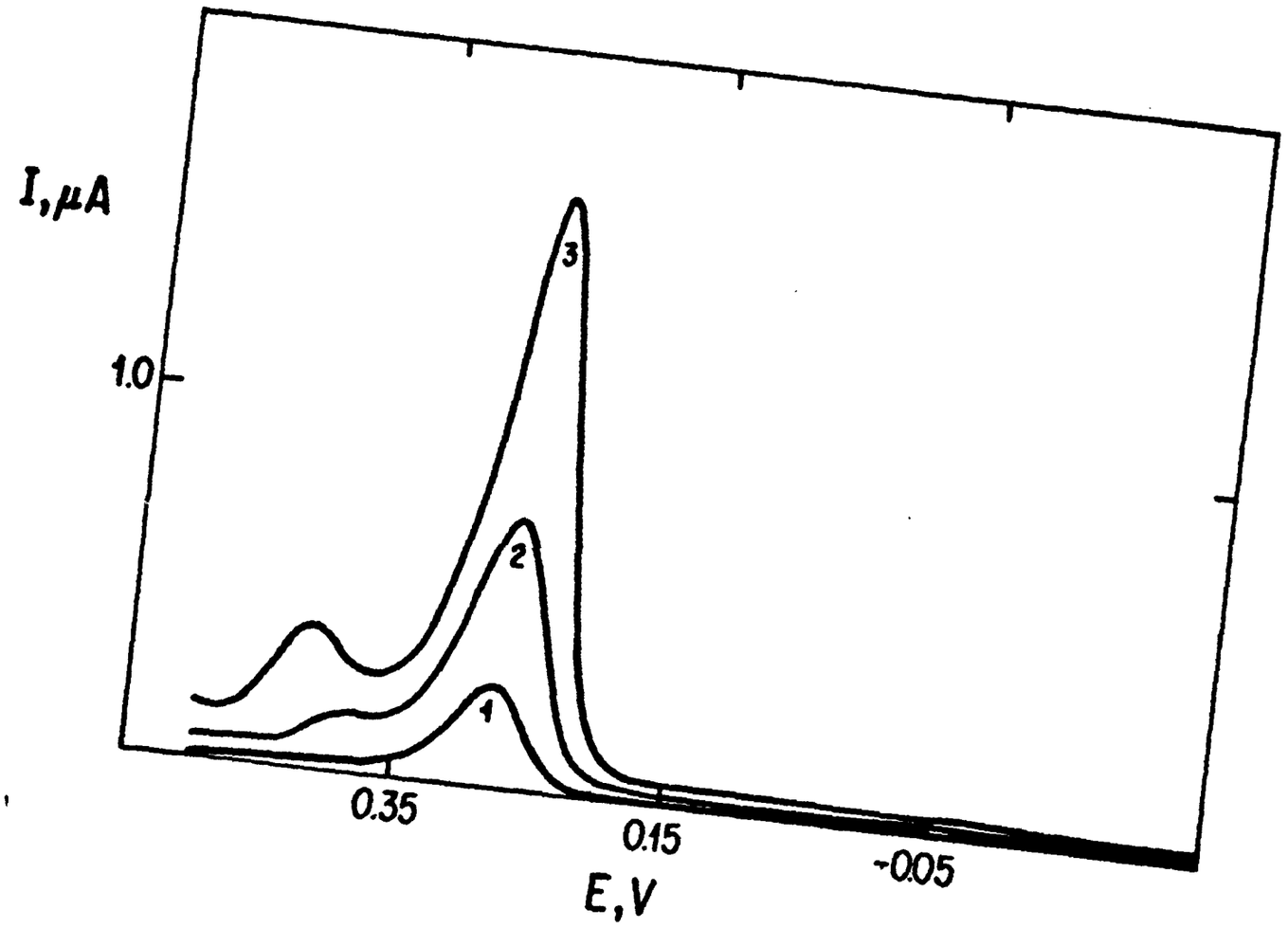

FIGURE 6A

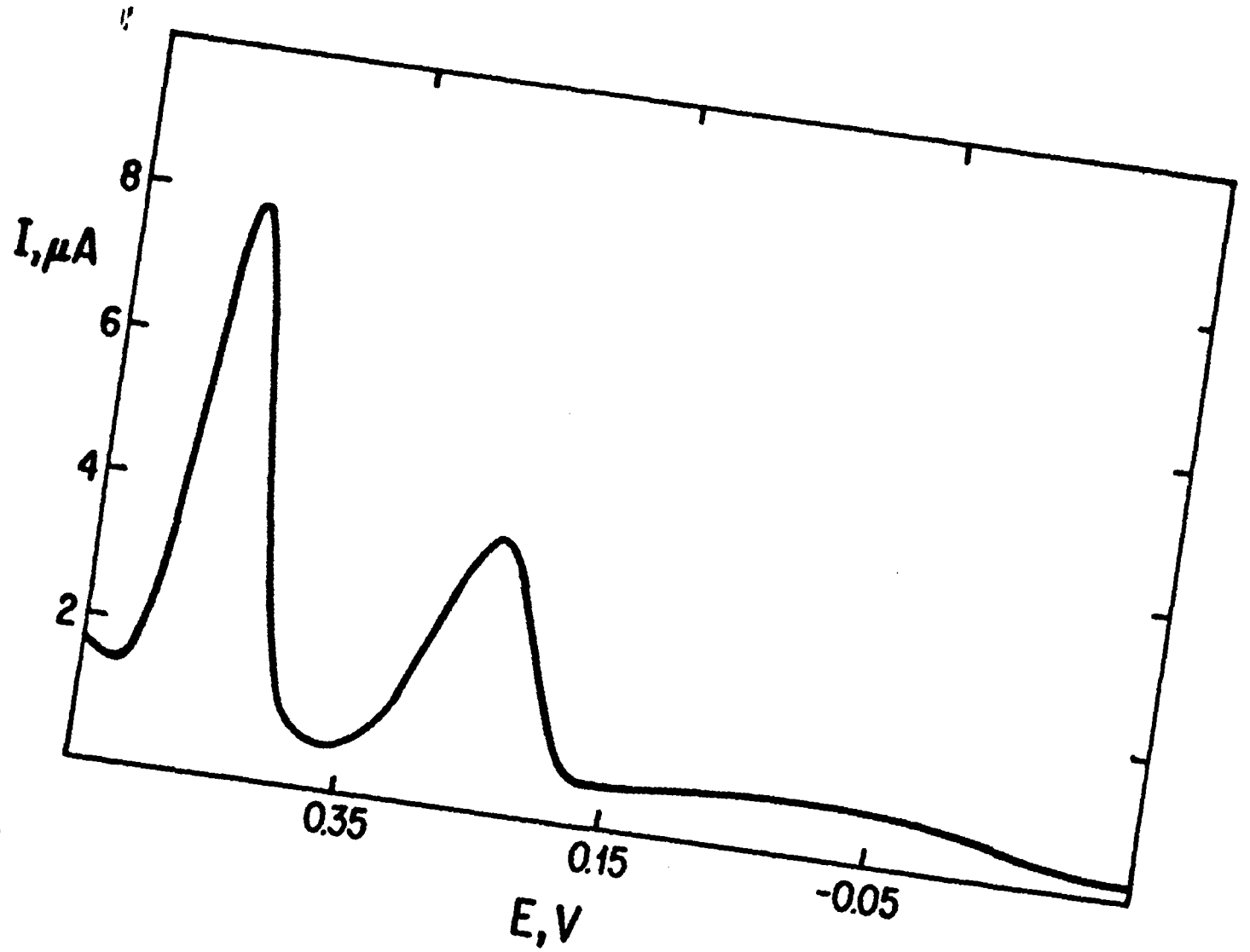

FIGURE 6B

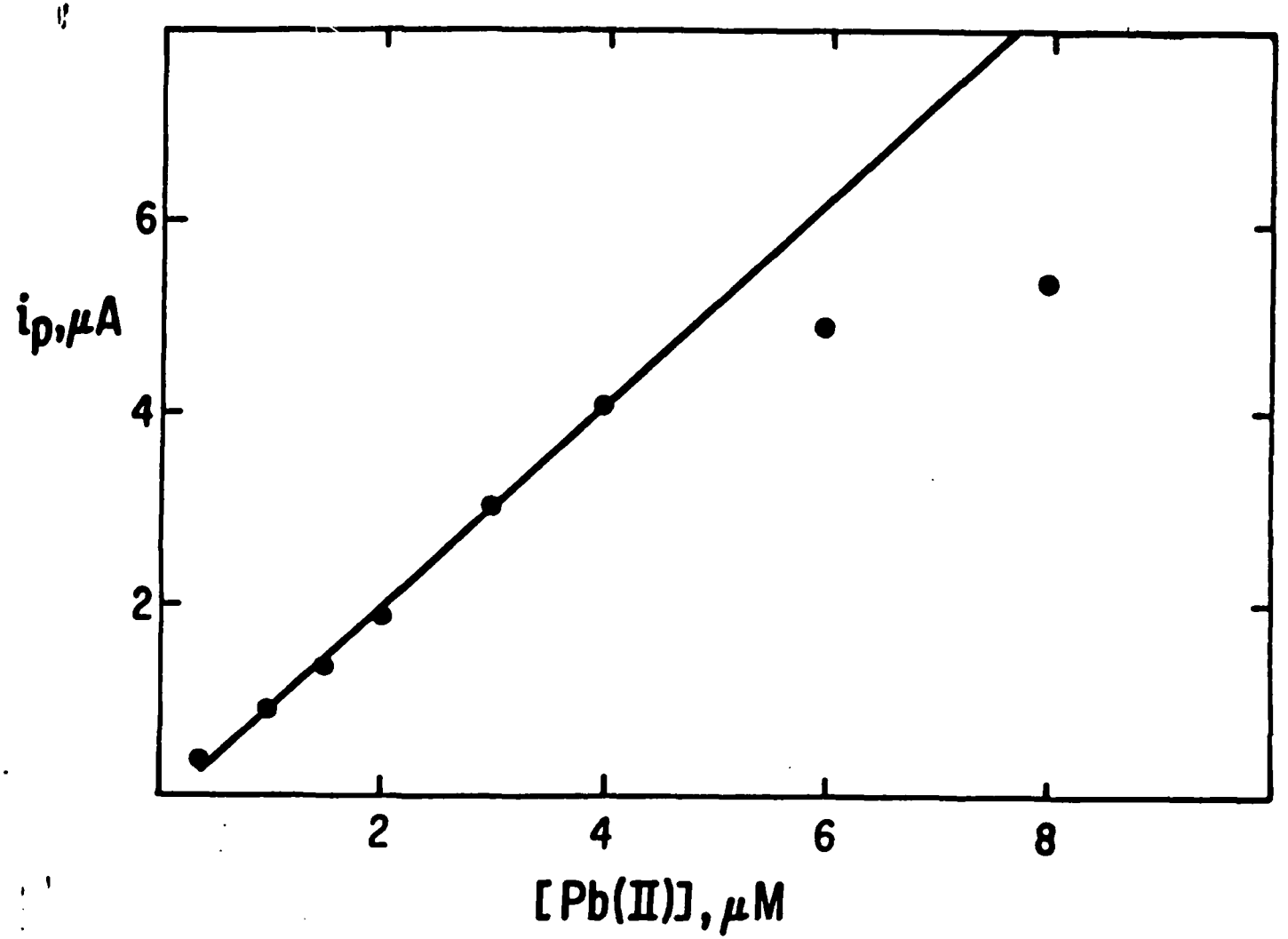

FIGURE 7

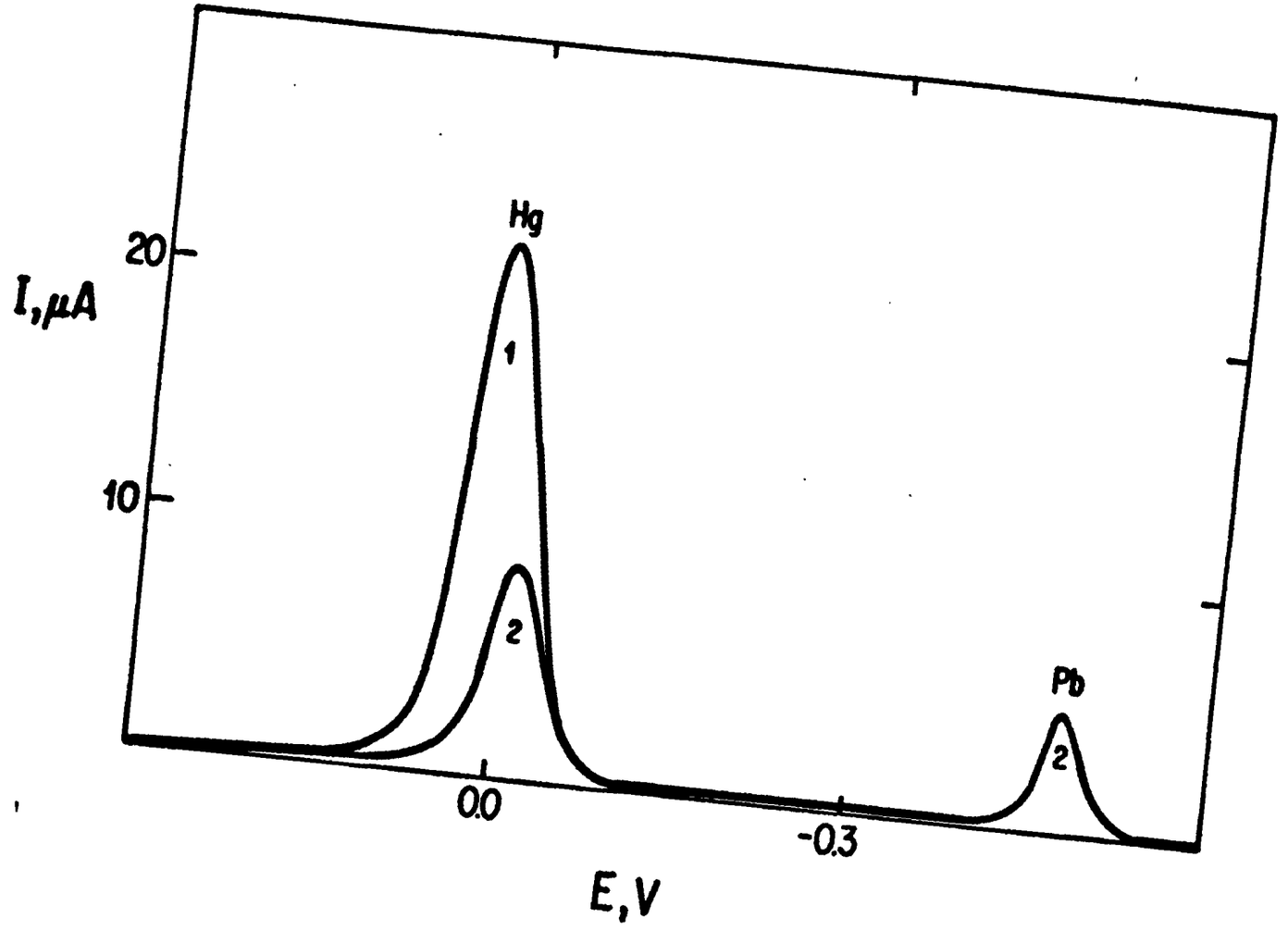

FIGURE 8

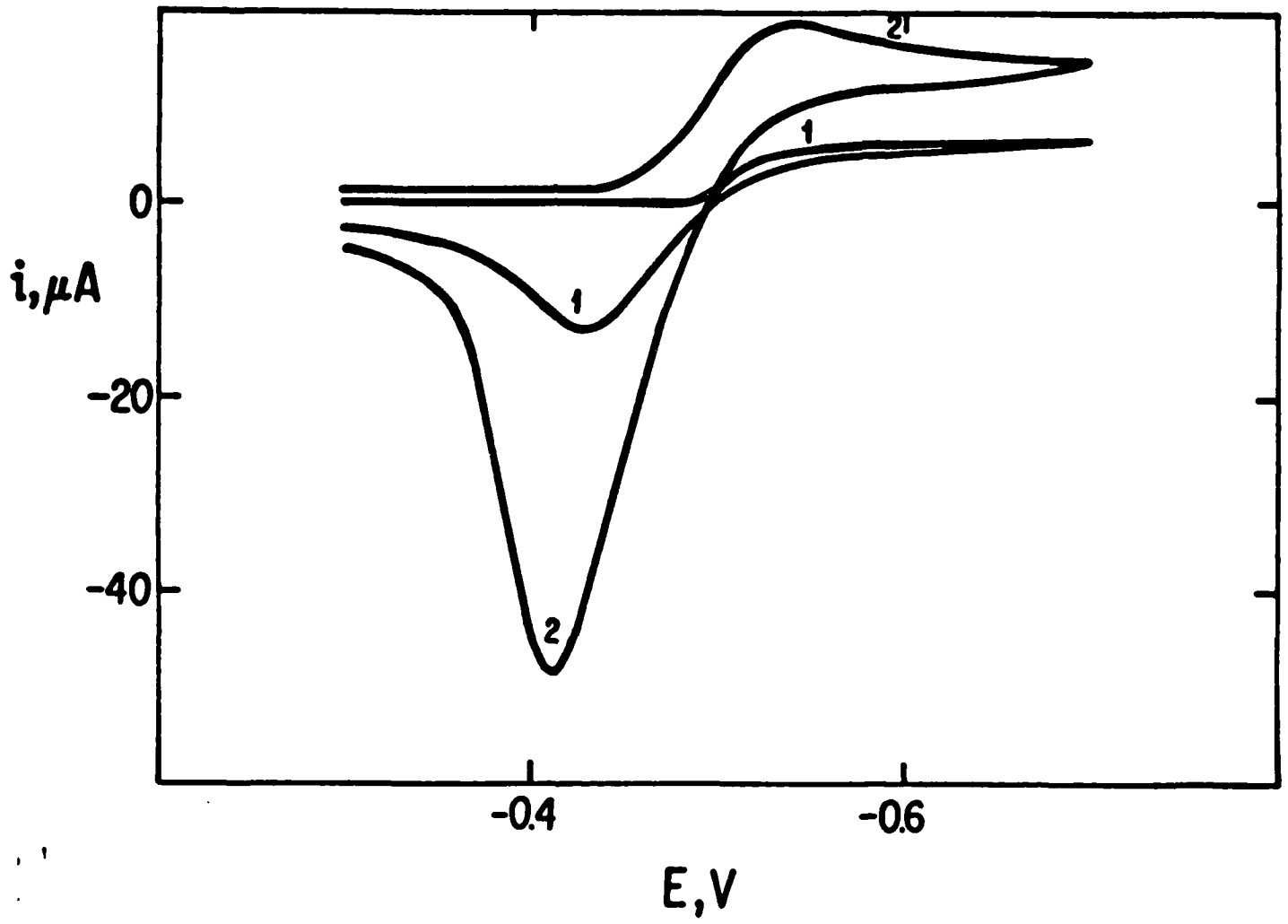

FIGURE 9

DL/413/83/01
GEN/413-2

TECHNICAL REPORT DISTRIBUTION LIST, GEN

	No. Copies
Office of Naval Research Attn: Code 413 800 N. Quincy Street Arlington, Virginia 22217	2
Dr. Bernard Douda Naval Weapons Support Center Code 5042 Crane, Indiana 47522	1
Commander, Naval Air Systems Command Attn: Code 310C (H. Rosenwasser) Washington, D.C. 20360	1
Naval Civil Engineering Laboratory Attn: Dr. R. W. Drisko Port Hueneme, California 93401	1
Defense Technical Information Center Building 5, Cameron Station Alexandria, Virginia 22314	12
DTNSRDC Attn: Dr. G. Bosmajian Applied Chemistry Division Annapolis, Maryland 21401	1
Dr. William Tolles Superintendent Chemistry Division, Code 6100 Naval Research Laboratory Washington, D.C. 20375	1
Dr. David Young Code 334 NORDA NSTL, Mississippi 39529	1
Naval Weapons Center Attn: Dr. A. B. Amster Chemistry Division China Lake, California 93555	1
Scientific Advisor Commandant of the Marine Corps Code RD-1 Washington, D.C. 20380	1
U.S. Army Research Office Attn: CRD-AA-IP P.O. Box 12211 Research Triangle Park, NC 27709	1
Mr. John Boyle Materials Branch Naval Ship Engineering Center Philadelphia, Pennsylvania 19112	1
Naval Ocean Systems Center Attn: Dr. S. Yamamoto Marine Sciences Division San Diego, California 91232	1

DL/413/83/01
051B/413-2

ABSTRACTS DISTRIBUTION LIST, 051B

Dr. R. A. Osteryoung
Department of Chemistry
State University of New York
Buffalo, New York 14214

Dr. J. Osteryoung
Department of Chemistry
State University of New York
Buffalo, New York 14214

Dr. B. R. Kowalski
Department of Chemistry
University of Washington
Seattle, Washington 98105

Dr. H. Chernoff
Department of Mathematics
Massachusetts Institute of Technology
Cambridge, Massachusetts 02139

Dr. A. Zirino
Naval Undersea Center
San Diego, California 92132

Dr. George H. Morrison
Department of Chemistry
Cornell University
Ithaca, New York 14853

Dr. Alan Bewick
Department of Chemistry
Southampton University
Southampton, Hampshire
ENGLAND SO9 5NH

Dr. M. B. Denton
Department of Chemistry
University of Arizona
Tucson, Arizona 85721

Dr. S. P. Perone
Lawrence Livermore National
Laboratory L-370
P.O. Box 808
Livermore, California 94550

Dr. G. M. Hieftje
Department of Chemistry
Indiana University
Bloomington, Indiana 47401

Dr. Christie G. Enke
Department of Chemistry
Michigan State University
East Lansing, Michigan 48824

Walter G. Cox, Code 3632
Naval Underwater Systems Center
Building 148
Newport, Rhode Island 02840

Professor Isiah M. Warner
Department of Chemistry
Emory University
Atlanta, Georgia 30322

Dr. Kent Eisentraut
Air Force Materials Laboratory
Wright-Patterson AFB, Ohio 45433

Dr. Adolph B. Amster
Chemistry Division
Naval Weapons Center
China Lake, California 93555

Dr. B. E. Douda
Chemical Sciences Branch
Code 50 C
Naval Weapons Support Center
Crane, Indiana 47322

Dr. John Eyler
Department of Chemistry
University of Florida
Gainesville, Florida 32611

DL/413/83/01
051B/413-2

ABSTRACTS DISTRIBUTION LIST, 051B

Professor J. Janata
Department of Bioengineering
University of Utah
Salt Lake City, Utah 84112

Dr. J. DeCorpo
NAVSEA
Code 05R14
Washington, D.C. 20362

Dr. Charles Anderson
Analytical Chemistry Division
Athens Environmental Laboratory
College Station Road
Athens, Georgia 30613

Dr. Ron Flemming
B 108 Reactor
National Bureau of Standards
Washington, D.C. 20234

Dr. Frank Herr
Office of Naval Research
Code 422CB
800 N. Quincy Street
Arlington, Virginia 22217

Professor E. Keating
Department of Mechanical Engineering
U.S. Naval Academy
Annapolis, Maryland 21401

Dr. M. H. Miller
1133 Hampton Road
Route 4
U.S. Naval Academy
Annapolis, Maryland 21401

Dr. Clifford Spiegelman
National Bureau of Standards
Room A337 Bldg. 101
Washington, D.C. 20234

Dr. Denton Elliott
AFOSR/NC
Bolling AFB
Washington, D.C. 20362

Dr. B. E. Spielvogel
Inorganic and Analytical Branch
P.O. Box 12211
Research Triangle Park, NC 27709

Ms. Ann De Witt
Material Science Department
160 Fieldcrest Avenue
Raritan Center
Edison, New Jersey 08818

Dr. A. Harvey
Code 6110
Naval Research Laboratory
Washington, D.C. 20375

Mr. S. M. Hurley
Naval Facilities Engineering Command
Code 032P
200 Stovall Street
Alexandria, Virginia 22331

Ms. W. Parkhurst
Naval Surface Weapons Center
Code R33
Silver Spring, Maryland 20910

Dr. M. Robertson
Electrochemical Power Sources Division
Code 305
Naval Weapons Support Center
Crane, Indiana 47522

Dr. Andrew T. Zander PI204
Perkin-Elmer Corporation
901 Ethan Allen Highway/MS905
Ridgefield, Connecticut 06877

DL/413/83/01
051B/413-2

ABSTRACTS DISTRIBUTION LIST, 051B

Dr. Marvin Wilkerson
Naval Weapons Support Center
Code 30511
Crane, Indiana 47522

Dr. J. Wyatt
Naval Research Laboratory
Code 6110
Washington, D.C. 20375

Dr. J. MacDonald
Code 6110
Naval Research Laboratory
Washington, D.C. 20375

Dr. H. Wohltjen
Naval Research Laboratory
Code 6170
Washington, D.C. 20375

Dr. John Hoffsommer
Naval Surface Weapons Center
Building 30 Room 208
Silver Spring, Maryland 20910

Dr. Robert W. Shaw
U.S. Army Research Office
Box 12211
Research Triangle Park, NC 27709

ABSTRACTS DISTRIBUTION LIST, 359/627

Dr. Paul Delahay
Department of Chemistry
New York University
New York, New York 10003

Dr. P. J. Hendra
Department of Chemistry
University of Southampton
Southampton SO9 5NH
United Kingdom

Dr. T. Katan
Lockheed Missiles and
Space Co., Inc.
P.O. Box 504
Sunnyvale, California 94088

Dr. D. N. Bennion
Department of Chemical Engineering
Brigham Young University
Provo, Utah 84602

Mr. Joseph McCartney
Code 7121
Naval Ocean Systems Center
San Diego, California 92152

Dr. J. J. Auborn
Bell Laboratories
Murray Hill, New Jersey 07974

Dr. Joseph Singer, Code 302-1
NASA-Lewis
21000 Brookpark Road
Cleveland, Ohio 44135

Dr. P. P. Schmidt
Department of Chemistry
Oakland University
Rochester, Michigan 48063

Dr. H. Richtol
Chemistry Department
Rensselaer Polytechnic Institute
Troy, New York 12181

Dr. R. A. Marcus
Department of Chemistry
California Institute of Technology
Pasadena, California 91125

Dr. E. Yeager
Department of Chemistry
Case Western Reserve University
Cleveland, Ohio 44106

Dr. C. E. Mueller
The Electrochemistry Branch
Naval Surface Weapons Center
White Oak Laboratory
Silver Spring, Maryland 20910

Dr. Sam Perone
Chemistry & Materials
Science Department
Lawrence Livermore National Laboratory
Livermore, California 94550

Dr. Royce W. Murray
Department of Chemistry
University of North Carolina
Chapel Hill, North Carolina 27514

Dr. B. Brummer
EIC Incorporated
111 Downey Street
Norwood, Massachusetts 02062

Dr. Adam Heller
Bell Laboratories
Murray Hill, New Jersey 07974

Electrochimica Corporation
Attn: Technical Library
2485 Charleston Road
Mountain View, California 94040

Library
Duracell, Inc.
Burlington, Massachusetts 01803

Dr. A. B. Ellis
Chemistry Department
University of Wisconsin
Madison, Wisconsin 53706

Dr. Manfred Breiter
Institut fur Technische Elektrochemie
Technischen Universitat Wien
9 Getreidemarkt, 1160Wien
AUSTRIA

6

ABSTRACTS DISTRIBUTION LIST, 359/627

Dr. M. Wrighton
Chemistry Department
Massachusetts Institute
of Technology
Cambridge, Massachusetts 02139

Dr. B. Stanley Pons
Department of Chemistry
University of Utah
Salt Lake City, Utah 84112

Donald E. Mains
Naval Weapons Support Center
Electrochemical Power Sources Division
Crane, Indiana 47522

S. Ruby
DOE (STOR)
M.S. 6B025 Forrestal Bldg.
Washington, D.C. 20595

Dr. A. J. Bard
Department of Chemistry
University of Texas
Austin, Texas 78712

Dr. Janet Osteryoung
Department of Chemistry
State University of New York
Buffalo, New York 14214

Dr. Donald W. Ernst
Naval Surface Weapons Center
Code R-33
White Oak Laboratory
Silver Spring, Maryland 20910

Mr. James R. Moden
Naval Underwater Systems Center
Code 3632
Newport, Rhode Island 02840

Dr. Bernard Spielvogel
U.S. Army Research Office
P.O. Box 12211
Research Triangle Park, NC 27709

Dr. Aaron Fletcher
Naval Weapons Center
Code 3852
China Lake, California 93555

Dr. M. M. Nicholson
Electronics Research Center
Rockwell International
3370 Miraloma Avenue
Anaheim, California

Dr. Michael J. Weaver
Department of Chemistry
Purdue University
West Lafayette, Indiana 47907

Dr. R. David Rauh
EIC Laboratories, Inc.
111 Downey Street
Norwood, Massachusetts 02062

Dr. Aaron Wold
Department of Chemistry
Brown University
Providence, Rhode Island 02192

Dr. Martin Fleischmann
Department of Chemistry
University of Southampton
Southampton SO9 5NH ENGLAND

Dr. R. A. Osteryoung
Department of Chemistry
State University of New York
Buffalo, New York 14214

Dr. Denton Elliott
Air Force Office of Scientific
Research
Bolling AFB
Washington, D.C. 20332

Dr. R. Nowak
Naval Research Laboratory
Code 6170
Washington, D.C. 20375

Dr. D. F. Shriver
Department of Chemistry
Northwestern University
Evanston, Illinois 60201

Dr. Boris Cahan
Department of Chemistry
Case Western Reserve University
Cleveland, Ohio 44106

ABSTRACTS DISTRIBUTION LIST, 359/627

Dr. David Aikens
Chemistry Department
Rensselaer Polytechnic Institute
Troy, New York 12181

Dr. A. B. P. Lever
Chemistry Department
York University
Downsview, Ontario M3J1P3

Dr. Stanislaw Szpak
Naval Ocean Systems Center
Code 6343, Bayside
San Diego, California 95152

Dr. Gregory Farrington
Department of Materials Science
and Engineering
University of Pennsylvania
Philadelphia, Pennsylvania 19104

M. L. Robertson
Manager, Electrochemical
and Power Sources Division
Naval Weapons Support Center
Crane, Indiana 47522

Dr. T. Marks
Department of Chemistry
Northwestern University
Evanston, Illinois 60201

Dr. Micha Tomkiewicz
Department of Physics
Brooklyn College
Brooklyn, New York 11210

Dr. Lesser Blum
Department of Physics
University of Puerto Rico
Rio Piedras, Puerto Rico 00931

Dr. Joseph Gordon, II
IBM Corporation
K33/281
5600 Cottle Road
San Jose, California 95193

Dr. Hector D. Abruna
Department of Chemistry
Cornell University
Ithaca, New York 14853

Dr. D. H. Whitmore
Department of Materials Science
Northwestern University
Evanston, Illinois 60201

Dr. Alan Bewick
Department of Chemistry
The University of Southampton
Southampton, S09 5NH ENGLAND

Dr. E. Anderson
NAVSEA-56Z33 NC #4
2541 Jefferson Davis Highway
Arlington, Virginia 20362

Dr. Bruce Dunn
Department of Engineering &
Applied Science
University of California
Los Angeles, California 90024

Dr. Elton Cairns
Energy & Environment Division
Lawrence Berkeley Laboratory
University of California
Berkeley, California 94720

Dr. D. Cipris
Allied Corporation
P.O. Box 3000R
Morristown, New Jersey 07960

Dr. M. Philpott
IBM Corporation
5600 Cottle Road
San Jose, California 95193

Dr. Donald Sandstrom
Boeing Aerospace Co.
P.O. Box 3999
Seattle, Washington 98124

Dr. Carl Kannewurf
Department of Electrical Engineering
and Computer Science
Northwestern University
Evanston, Illinois 60201

Dr. Richard Pollard
Department of Chemical Engineering
University of Houston
4800 Calhoun Blvd.
Houston, Texas 77004

DL/413/83/01
359/413-2

ABSTRACTS DISTRIBUTION LIST, 359/627

Dr. Robert Somoano
Jet Propulsion Laboratory
California Institute of Technology
Pasadena, California 91103

Dr. Johann A. Joebstl
USA Mobility Equipment R&D Command
DRDME-EC
Fort Belvoir, Virginia 22060

Dr. Judith H. Ambrus
NASA Headquarters
M.S. RTS-6
Washington, D.C. 20546

Dr. Albert R. Landgrebe
U.S. Department of Energy
M.S. 6B025 Forrestal Building
Washington, D.C. 20595

Dr. J. J. Brophy
Department of Physics
University of Utah
Salt Lake City, Utah 84112

Dr. Charles Martin
Department of Chemistry
Texas A&M University
College Station, Texas 77843

Dr. H. Tachikawa
Department of Chemistry
Jackson State University
Jackson, Mississippi 39217

Dr. Theodore Beck
Electrochemical Technology Corp.
3935 Leary Way N.W.
Seattle, Washington 98107

Dr. Farrell Lytle
Boeing Engineering and
Construction Engineers
P.O. Box 3707
Seattle, Washington 98124

Dr. Robert Gotscholl
U.S. Department of Energy
MS G-226
Washington, D.C. 20545

Dr. Edward Fletcher
Department of Mechanical Engineering
University of Minnesota
Minneapolis, Minnesota 55455

Dr. John Fontanella
Department of Physics
U.S. Naval Academy
Annapolis, Maryland 21402

Dr. Martha Greenblatt
Department of Chemistry
Rutgers University
New Brunswick, New Jersey 08903

Dr. John Wasson
Syntheco, Inc.
Rte 6 - Industrial Pike Road
Gastonia, North Carolina 28052

Dr. Walter Roth
Department of Physics
State University of New York
Albany, New York 12222

Dr. Anthony Sammells
Eltron Research Inc.
4260 Westbrook Drive, Suite 111
Aurora, Illinois 60505

Dr. W. M. Risen
Department of Chemistry
Brown University
Providence, Rhode Island 02192

Dr. C. A. Angell
Department of Chemistry
Purdue University
West Lafayette, Indiana 47907

Dr. Thomas Davis
Polymer Science and Standards
Division
National Bureau of Standards
Washington, D.C. 20234

Ms. Wendy Parkhurst
Naval Surface Weapons Center R-33
Silver Spring, Maryland 20910

END

1-87

DTIC